Co-published by
Institute of Fluid-Flow Machinery
Polish Academy of Sciences
Committee on Thermodynamics and Combustion
Polish Academy of Sciences

http://www.imp.gda.pl/archives-of-thermodynamics/

ARCHIVES OF THERMODYNAMICS

Mixed convection flow in a porous channel under the effects of exothermic chemical reactions and local thermal non-equilibrium

Camelia Berghian-Grosan[a], Rares Serban Pop[b], Teodor Silviu Grosan[c*]

[a]National Institute for Research and Development of Isotopic and Molecular Technologies, Donat 67-103, 400293 Cluj-Napoca, Romania
[b]University of Chester, School of Computer and Engineering Sciences, Parkgate Road, Chester, CH1 4BJ, United Kingdom
[c]Babes-Bolyai University, Department of Mathematics, M. Kogalniceanu 1, 400084 Cluj-Napoca, Romania
*Corresponding author email: teodor.grosan@ubbcluj.ro

Received: 09.04.2024; revised: 02.07.2024; accepted: 03.12.2024

Abstract

The effect of a first-order exothermic chemical reaction on the mixed flow in a vertical channel filled with a porous medium has been studied using the local thermal non-equilibrium model. A mathematical model including the exponential term for heat generation in the fluid phase and interphase heat transfer terms in both the fluid and solid phases was considered. The above dimensionless model has been solved numerically using the Matlab routine bvp4c for the energy equations together with an in-house developed code for the momentum equation. The existence of dual solutions is reported for certain values of the Frank-Kamenetskii number. The obtained profiles of temperature and velocity have been plotted. In addition, the ranges of existence of the dual solutions are reported.

Keywords: Fully developed flow; Local thermal non-equilibrium; Exothermic chemical reaction

Vol. 45(2024), No. 4, 237–242; doi: 10.24425/ather.2024.152013

Cite this manuscript as: Berghian-Grosan, C., Pop, R.S., & Grosan, T.S. (2024). Mixed convection flow in a porous channel under the effects of exothermic chemical reactions and local thermal non-equilibrium. *Archives of Thermodynamics*, 45(4), 237–242.

1. Introduction

Thermal non-equilibrium between solid and fluid phases in porous media is an important effect which is usually present when high-speed flows are involved or height porosities are present, see Vafai and Sozen [1] and Kuznetsov and Vafai [2]. Such situations are related to the study of nuclear reactor cores and in hypothetical nuclear reactor accidents, chemical reactors, etc. (see Nield and Bejan, [3]). Detailed reviews of mathematical models of heat transfer in porous media, when the thermal non-equilibrium is present, can be found in Kuznetsov [4,5]. Rees and Pop [6,7] performed a numerical and analytical study on the free convective boundary-layer flow and stagnation-point flow when the thermal non-equilibrium is taken into account. They reported that, when the solid matrix and the filling fluid are not in local thermal equilibrium, the behaviour of the flow is modified substantially. Baytas and Pop [8] studied free convection in a differentially heated square cavity using a thermal non-equilibrium model for heat transfer and the Darcy model for fluid flow. Compared to the case of thermal equilibrium, lower values of the Nusselt number were obtained in the case of thermal non-equilibrium. These values also depend on the interphase heat transfer parameters.

Self-ignition or thermal explosion can occur in heat transfer problems (e.g. in storage technology) due to chemical exothermic reactions. Such undesirable behaviour can be described using the mathematical model given by Semenov [9]. The appearance of the self-ignition/explosion is characterized by the Frank-Kamenetskii number. Critical values of this number, at which the impact occurs, are reported by Lazarovici et al. [10] for a ca-

Nomenclature

a – concentration of reactant A in Eq. (6)
c – specific heat at constant pressure, J kg^{-1}K^{-1}
Da – Darcy number
E – activation energy, J
g – gravitational acceleration, m^{2}s^{-1}
Gr – Grashof number
h – interphase heat transfer coefficient, W m^{-2}K^{-1}
H – modified inter-phase heat transfer parameter,
k – thermal conductivity, W m^{-1}K^{-1}
k_0 – pre-exponential factor
K – Frank-Kamenestkii number
K_c – critical Frank-Kamenestkii number
$\tilde{K}$ – permeability, m^2
L – characteristic length, m
N – grid dimension
p – pressure, N m^{-2}
P – dimensionless pressure
Q – exothermicity of reaction, J mol^{-1}
r_T – dimensionless value of the temperature on the boundary
R – universal gas constant, J mol^{-1}K^{-1}
Re – Reynolds number
T – temperature, K
T_0 – reference temperature, K
u, v – filtration velocity components, m s^{-1}
U – dimensionless filtration velocity
U_0 – reference velocity, m s^{-1}
x, y – Cartesian coordinates, m
X, Y – dimensionless Cartesian coordinates

Greek symbols

β – volumetric thermal expansion coefficient, K^{-1}
γ – dimensionless pressure gradient
θ – dimensionless temperature
θ' – derivative of the dimensionless temperature with respect to y
κ – thermal conductivities ratio
λ – dimensionless mixed convection parameter
μ – dynamic viscosity, kg m s^{-1}
$\tilde{\mu}$ – effective dynamic viscosity, kg m s^{-1}
μ^* – viscosities ratio
ρ – density, kg m^{-3}
ϕ – porosity

Subscripts and Superscripts

f – fluid phase
s – solid phase

vity filled with a porous medium under local thermal equilibrium conditions.

The effect of heat generated by exothermic reactions in porous media in a state of local thermal non-equilibrium has not yet been studied. Therefore, in this work, we will deal with the analysis of the effect of heat generated by an exothermic chemical reaction on the flow and heat transfer in a porous medium that is in a state of thermal non-equilibrium.

2. Mathematical model

We consider the mixed convection flow and heat transfer in the presence of exothermic chemical reactions in a vertical channel filled by a fluid porous medium (see Fig. 1). The mathematical model for convective flow in a porous medium, using the Darcy-Brinkman formulation, and considering the thermal non-equilibrium is given in [8], while details of the heat generation term due to an exothermic chemical reaction can be found in [10]. On the boundaries, the fluid and solid phases are assumed to be in local

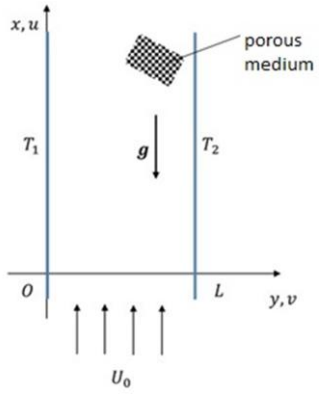

Fig. 1. Geometry of the problem.

thermal equilibrium ($T_f = T_s$). Thus, for the governing equations, a combined two temperatures model is used, considering that the heat is generated in the fluid phase. The equations of continuity, momentum and energy for fluid and solid phases are:

$$\frac{\partial u}{\partial x} + \frac{\partial v}{\partial y} = 0, \tag{1}$$

$$\frac{\partial p}{\partial x} = -\frac{\mu}{\tilde{K}} u + \tilde{\mu} \nabla^2 u + \rho g \, \beta \left(T_f - T_0\right), \tag{2}$$

$$\frac{\partial p}{\partial y} = -\frac{\mu}{\tilde{K}} v + \tilde{\mu} \, \nabla^2 v, \tag{3}$$

$$(\rho \, c)_f \left(u \frac{\partial T_f}{\partial x} + v \frac{\partial T_f}{\partial y}\right) =$$

$$= \phi k_f \left(\frac{\partial^2 T_f}{\partial x^2} + \frac{\partial^2 T_f}{\partial y^2}\right) + h\left(T_f - T_s\right) + Q k_0 a \, \mathrm{e}^{-E/RT_f}, \tag{4}$$

$$0 = (1 - \phi) k_s \left(\frac{\partial^2 T_s}{\partial x^2} + \frac{\partial^2 T_s}{\partial y^2}\right) + h\left(T_f - T_s\right). \tag{5}$$

In Eqs. (1) to (5), u and v are the components of the Darcian velocity, p is the pressure, T_f is the temperature of the fluid phase and T_s is the temperature of the solid phase. The physical properties of the fluid are given in Nomenclature.

Following the Arrhenius kinetics (see [10]) where the reactant A is transformed in the product B

$$A \rightarrow B + \text{heat}, \quad \text{rate} = k_0 a \, \mathrm{e}^{-E/RT}, \tag{6}$$

and the heat generated by a first order exothermic chemical reaction in the fluid phase is expressed by adding the term $Q k_0 a \, \mathrm{e}^{-E/RT_f}$ in Eq. (4).

Next, we assume that the process takes place far from the channel entrance and that the flow is fully developed, see Aung and Worku [11]:

$$v = 0, \quad \frac{\partial u}{\partial x} = 0, \quad \frac{\partial T}{\partial x} = 0, \quad \frac{\partial p}{\partial y} = 0, \quad \frac{\partial p}{\partial x} = \frac{dp}{dx} = \text{const.} \quad (7)$$

Thus, using assumptions (7) in Eqs. (1) to (5), the governing equations are:

$$\frac{dp}{dx} = -\frac{\mu}{\tilde{K}}u + \tilde{\mu}\,\frac{d^2u}{dy^2} + \rho g\,\beta\left(T_f - T_0\right), \quad (8)$$

$$0 = \phi k_f \frac{d^2T}{dy^2} + h\left(T_s - T_f\right) + Qk_0 a\, e^{-E/RT_f}, \quad (9)$$

$$0 = (1-\phi)k_s \frac{d^2T_s}{dy^2} + h\left(T_f - T_s\right), \quad (10)$$

along with the boundary conditions:

$$\begin{gathered} u = 0 \quad \text{at } y = 0 \quad \text{and} \quad y = L, \\ T_f = T_s = T_1 \quad \text{at } y = 0, \\ T_f = T_s = T_2 \quad \text{at } y = L, \\ T_1 > T_2. \end{gathered} \quad (11)$$

In order to solve Eqs. (8)–(11) and find the pressure gradient $\frac{dp}{dx}$, it is necessary to add a new equation related to the conservation of mass flow rate (see, Aung and Worku [11] and Cimpan [12]):

$$\int_0^L u dy = M = U_0 L. \quad (12)$$

By using the following dimensionless variables in Eqs. (8)–(12):

$$X = \frac{x}{\mathrm{Re}L}, \quad Y = \frac{y}{L}, \quad U = \frac{u}{U_0}, \quad P = \frac{p}{\rho U_0^2}, \quad \theta_f = \frac{T_f - T_0}{RT_0^2/E},$$
$$\theta_s = \frac{T_s - T_0}{RT_0^2/E}, \quad \mathrm{Re} = \frac{U_0 L}{\nu}, \quad T_0 = \frac{T_1 + T_2}{2}, \quad (13)$$

the mathematical model in the dimensionless form is obtained:

$$\gamma = -\frac{1}{\mathrm{Da}}U + \mu^* \frac{d^2U}{dY^2} + \lambda\theta_f, \quad (14)$$

$$0 = \frac{d^2\theta_f}{dY^2} + H\left(\theta_s - \theta_f\right) + \mathrm{K}\, e^{\theta_f}, \quad (15)$$

$$0 = \frac{d^2\theta_s}{dY^2} + \kappa H\left(\theta_f - \theta_s\right), \quad (16)$$

$$\begin{gathered} U = 0 \quad \text{at } Y = 0 \quad \text{and} \quad Y = 1, \\ \theta_f = \theta_s = r_T \quad \text{at } Y = 0, \\ \theta_f = \theta_s = -r_T \quad \text{at } Y = 1, \end{gathered} \quad (17)$$

$$\int_0^1 U dY = 1. \quad (18)$$

The governing parameters in Eqs. (14)–(17) are:

$\gamma = \frac{dP}{dX}$ (dimensionless pressure gradient),

$\mathrm{Da} = \frac{\tilde{K}}{L^2}$ (Darcy number),

$\mu^* = \frac{\tilde{\mu}}{\mu}$ (viscosities ratio in the Brinkman model),

$\lambda = \frac{\mathrm{Gr}}{\mathrm{Re}}$ (mixed convection parameter),

$\mathrm{Gr} = \frac{g\beta\left(\frac{RT_0^2}{E}\right)L^3}{\nu^2}$ (Grashof number),

$\mathrm{K} = \frac{Qk_0 aL^2}{\phi k_f\left(\frac{RT_0^2}{E}\right)}\, e^{-\frac{E}{RT_0}}$ (Frank-Kamenestkii number),

$\kappa = \frac{\phi k_f}{(1-\phi)k_s}$ (thermal conductivity ratio),

$r_T = \frac{T_1 - T_2}{2RT_0^2/E}$ (boundary condition parameter).

Assuming a large activation energy $\left(\frac{RT_0}{E} \ll 1\right)$, a Taylor expansion was used to derive the energy equation for the fluid phase, Eq. (15). Here, the Frank-Kamenestkii number K measures the heat produced by the reaction relative to its loss by Newtonian cooling and is responsible for the occurrence of the thermal explosion/ignition, see [10].

3. Numerical solution and results

We have solved the system of Eqs. (15) and (16) using the routine *bvp4c* from Matlab, using a prescribed error set to 10^{-9}. This routine uses a collocation method on a non-uniform mesh to solve boundary value problems. The method requires an initial mesh and an initial approximate solution, then during the solution process the error is estimated at each subinterval, and the mesh is adjusted to achieve the convergence. The energy equation (15) is very close to the well-known Bratu's equation [13], where $\theta(0) = \theta(1) = 0$. Similar to [13], it was found that there is a critical value of the parameter $\mathrm{K}_c(r_T, H, \kappa)$, which is the point of thermal explosion.

For $0 < \mathrm{K} < \mathrm{K}_c$, there are two solutions for the temperature θ_f, for $\mathrm{K} = \mathrm{K}_c$, we have one solution (for this value the explosion occurs), and for $\mathrm{K} > \mathrm{K}_c$, the equation has no solution. Following [13,14], we can conclude that the lower solution is the stable one. In the particular case of local thermal equilibrium, the obtained critical values K_c were compared with those obtained by Petrusel et al. [15] (for $r_T = 0$) and Pop et al. [14], see Table 1. Increasing the value of the parameter r_T leads to a reduction of the solution domain.

Next, we study the effect of local thermal nonequilibrium on the existence of the solutions of Eqs. (15) and (16). The values, for the modified interphase heat transfer parameter and the thermal conductivity ratio, were chosen on the basis of the paper by

Table 1. Values of the critical Frank-Kamenetskii number for different values of the parameter r_T.

r_T	K_c		
	Petrusel et al. [14]	Pop et al. [15]	Present
0	3.513830719	–	3.513959
0.1	–	3.51	3.510533
0.5	–	3.419	3.419371
1	–	3.155	3.155131
2	–	2.332	2.332904

Baytas and Pop [8]. The effect of varying the parameters H and κ on the range of existence of solutions is shown in Figs. 2 to 5.

The variation of the stable temperature profiles of the two phases (fluid phase and solid phase) with the boundary condition parameter r_T are given in Figs. 6 and 7. The maximum value of the temperature increases with the increase of r_T. For large values of r_T, there is an overshoot of the left boundary condition value for the θ_f profile. The same effect on the temperature profiles is observed for large values of the Frank-Kamenetskii number K, see Figs. 8 and 9.

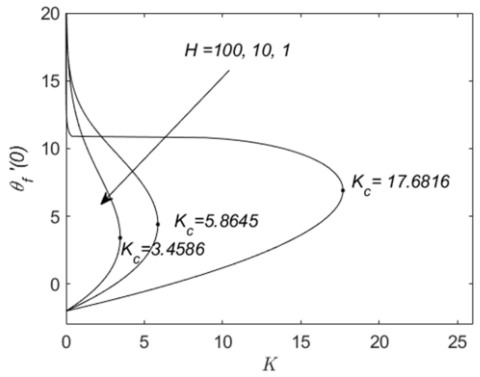

Fig. 2. Existence of dual solution and values of $\theta_f'(0)$ for different values of H when $r_T = 1$ and $\kappa = 0.1$.

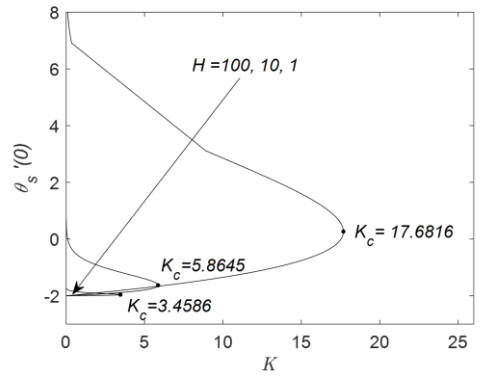

Fig. 3. Existence of dual solution and values of $\theta_s'(0)$ for different values of H when $r_T = 1$ and $\kappa = 0.1$.

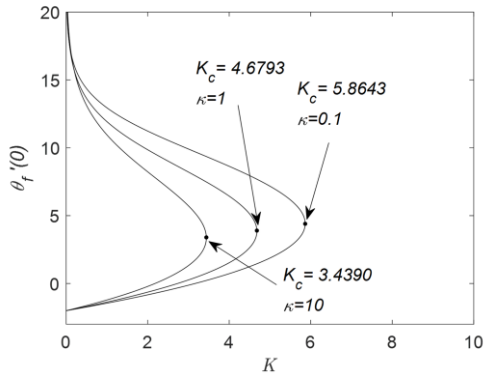

Fig. 4. Existence of dual solution and values of $\theta_f'(0)$ for different values of κ when $r_T = 1$ and $H = 10$.

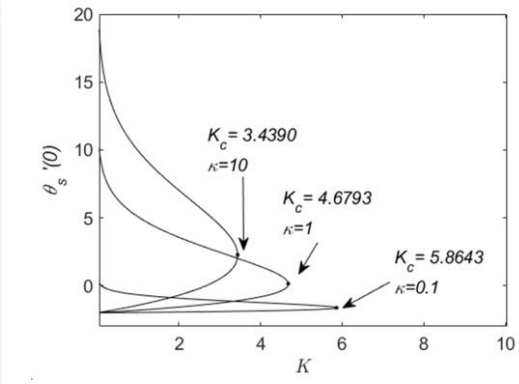

Fig. 5. Existence of dual solution and values of $\theta_s'(0)$ for different values of κ when $r_T = 1$ and $H = 10$.

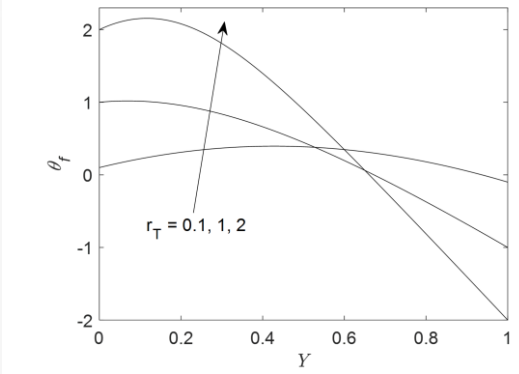

Fig. 6. Profiles of $\theta_f(Y)$ for different values of r_T when $\kappa = 2$, $H = 10$ and K = 3.

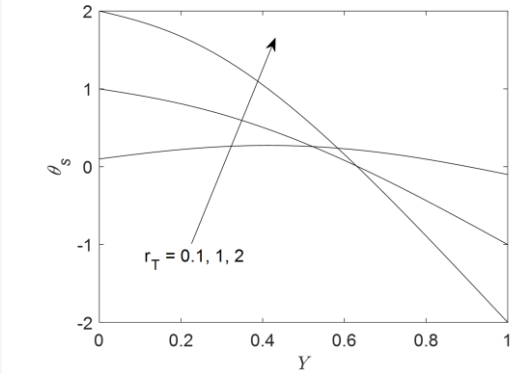

Fig. 7. Profiles of $\theta_s(Y)$ for different values of r_T when $\kappa = 2$, $H = 10$ and K = 3.

With the temperature profile obtained by solving the system of Eqs. (15) to (17), we focus on the solution of the momentum equation (14) along with the boundary conditions (17). The momentum equation was discretized using central finite differences on a uniform grid of dimension N. In addition, for the mass flux conservation equation, a midpoint quadrature formula was used. The obtained system of algebraic equations was solved using an in situ-built program using Matlab routines. In order to choose the size of the grid, a dependence simulation (see Table 2) was

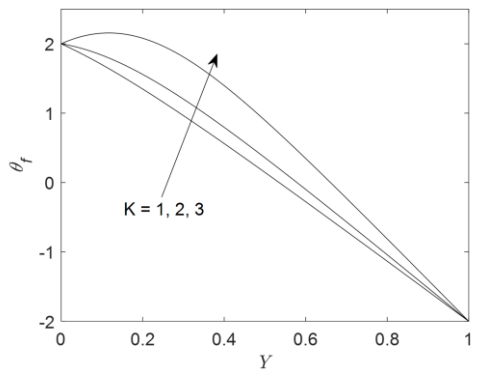

Fig. 8. Profiles of $\theta_f(Y)$ for different values of K when $\kappa = 2$, $H = 10$ and $r_T = 2$.

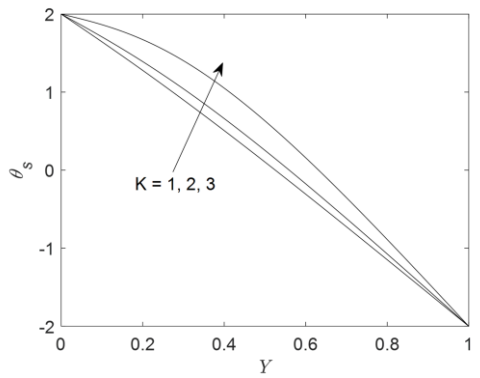

Fig. 9. Profiles of $\theta_s(Y)$ for different values of K when $\kappa = 2$, $H = 10$ and $r_T = 2$.

performed for the following values of the involved parameters: H = 10, K = 4, κ = 1, r_T = 1, λ = 1000, μ^* = 6, and Da = 10^{-2}. According to the results obtained, the numerical simulations are further carried out using a grid of dimension N = 401.

Profiles of the velocity were obtained for some typical values of the involved parameters. In this problem, the value of the viscosity ratio parameter was fixed, μ^* = 6, see Gentile and Straughan [16]. The effect of variation of parameters Da and λ on the mixed convective fully developed flow is well known. Thus, for fixed values of the flow parameters, Da = 10^{-3} and λ = 1000, we focused on the study of the effect of thermal parameters on the velocity profiles.

In Fig 10, the variation of the velocity profile with the parameter r_T is depicted. For large values of the parameter r_T, we notice the presence of the reverse flow near the cold (right) wall. Large values of r_T imply a large temperature difference between the left and right walls, and this leads to negative buoyancy forces near the cold wall, which determine the reverse flow.

Next, in order to study the effect of the interphase heat transfer parameter H on the flow, computational simulations were performed for H = 1, 10, and 100. The increase of the value of H leads to an increase of the maximum values of the velocity; the reverse flow is more visible for large values of H near the right (cold) wall, see Fig 11.

The effect of the thermal conductivities ratio κ on the velocity is shown in Fig. 12. The magnitude of U increases slowly with the increase of κ. Finally, the variation of velocity profiles with the parameter K is presented in Fig. 13. The convective flow is augmented by the increase of K due to the higher profile of temperature, see Fig. 8. The increase of the parameter also intensifies the reverse flow.

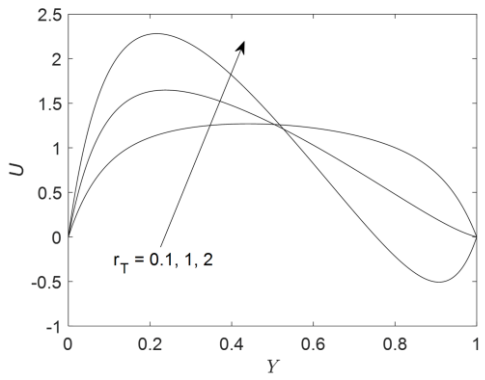

Fig. 10. Variation of velocity profiles U with r_T for K = 4, $H = 10$, $\kappa = 2$.

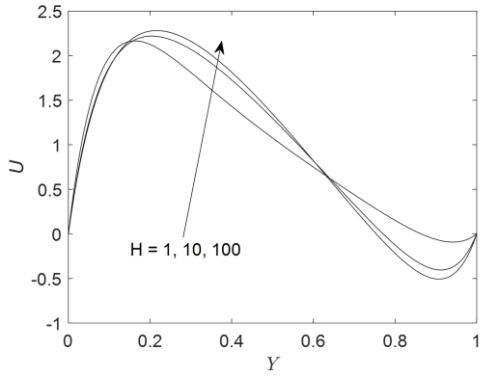

Fig. 11. Variation of velocity profiles U with H for $r_T = 2$, K = 4, $\kappa = 2$.

Table 2. Grid dependence test.

Grid dimension, N	max(U)	γ
101	3.206797	295.004812
201	3.206853	294.984245
401	3.206974	294.979059
2001	3.206979	294.977760

4. Conclusions

The effect of first order exothermic chemical reactions on the mixed convective flow in a porous medium was studied considering a thermal non-equilibrium model.

- The solution of the energy equation depends on the Frank-Kamenestkii number, K. For 0 < K < K_c (critical number), there are two solutions, for K = K_c, we have one solution and for K > K_c, the equation has no solution.

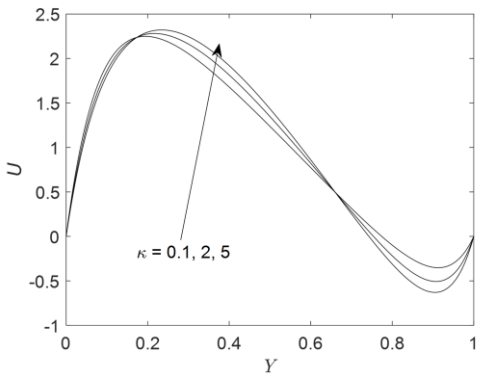

Fig. 12. Variation of velocity profiles U with κ for $r_T = 2,\ H = 10,\ K = 3$.

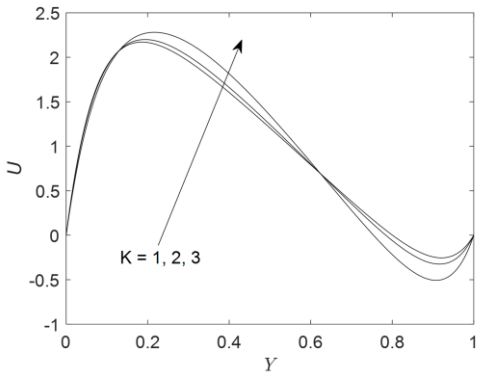

Fig. 13. Variation of velocity profiles U with K for $r_T = 2,\ H = 10,\ \kappa = 2$.

- The increase of the r_T parameter determines the apparition of the reverse flow near the cold wall.
- The magnitude of U increases with the increase of the heat transfer parameters H and κ.
- For more realistic physical modelling of the ignition/explosion occurrence, unsteady effects can be considered [17,18], while for sparse porous media Darcy-Forchheimer or Brinkman mathematical models have to be used [19].

Acknowledgements

The authors would like to acknowledge the financial support received from the grant PN-III-P4-PCE-2021-0993 (contract PCE 69/2022), UEFISCDI (Romanian Ministry of Sciences).

References

[1] Vafai, K., & Sozen, M. (1990). Analysis of energy and momentum transport for fluid flow through a porous bed. *ASME Journal of Heat Transfer*, 112(3), 690–699. doi: 10.1115/1.2910442

[2] Kuznetsov, A.V., & Vafai, K. (1995). Analytical comparison and criteria for heat and mass transfer models in metal hydride packed beds. *International Journal of Heat and Mass Transfer*, 38(15), 2873–2884. doi: 10.1016/0017-9310(94)00331-O

[3] Nield, D.A., & Bejan, A. (2017). *Convection in Porous Media.* Springer.

[4] Kuznetsov, A.V. (1996). A perturbation solution for a non thermal equilibrium fluid flow through a three dimensional sensible storage packed bed. *ASME Journal of Heat Transfer*, 118(2), 508–510. doi: 10.1115/1.2825881

[5] Kuznetsov, A.V. (1998) Thermal nonequilibrium forced convection in porous media. In *Transport Phenomena in Porous Media*, (pp. 103–129). Pergamon Oxford.

[6] Rees, D.A.S., & Pop, I. (1999). Free convective stagnation-point flow in a porous medium using a thermal nonequilibrium model. *International Communications in Heat and Mass Transfer*, 26(7), 945–954. doi: 10.1016/S0735-1933(99)00084-6

[7] Rees, D.A.S., & Pop, I. (2000). Vertical free convective boundary-layer flow in a porous medium using a thermal nonequilibrium model. *Journal on Porous Media*, 3(1), 31–44. doi: 10.1615/JPorMedia.v3.i1.30

[8] Baytas, A.C., & Pop, I. (2002). Free convection in a square porous cavity using a thermal nonequilibrium model. *International Journal of Thermal Sciences*, 41(9) 861–870. doi: 10.1016/S1290-0729(02)01379-0

[9] Semenov, N.N. (1940). Thermal theory of combustion and explosion. III Theory of normal flame propagation. *Progress of Physical Science*, 24 (4).

[10] Lazarovici, A. Volpert, V., & Merkin, J.H. (2005). Steady states, oscillations and heat explosion in a combustion problem with convection. *European Journal of Mechanics B/Fluids*, 24(2), 189–203. doi: 10.1016/j.euromechflu.2004.06.007

[11] Aung, W., & Worku, G. (1986). Developing flow and flow reversal in a vertical channel with asymmetric wall temperatures. *ASME Journal of Heat Transfer*, 108(2), 299−304. doi: 10.1115/1.3246919

[12] Cimpean, D.S. (2022). Dynamics of colloidal mixture of Cu-Al_2O_3/water in an inclined porous channel due to mixed convection: Significance of entropy generation. *Coatings*, 12(9), 1347. doi: 10.3390/coatings12091347

[13] Bratu, G. (1914). Sur les équations intégrales non linéaires. *Bulletin de la Société Mathématique de France,*, 42, 113−142. doi: 10.24033/bsmf.943

[14] Pop, I., Grosan, T., & Revnic, C. (2010). Effect of heat generated by an exothermic reaction on the fully developed mixed convection flow in a vertical channel. *Communications in Nonlinear Science and Numerical Simulation*, 15(3), 471–474. doi: 10.1016/j.cnsns.2009.04.010

[15] Petrusel, A., Rus, I.A., & Serban, M.A. (2021). Theoretical and numerical considerations on Bratu-type problems. *Studia Universitatis Babes-Bolyai Matematica*, 66(1), 29–46. doi: 10.24193/subbmath. 2021.1.03

[16] Gentile, M., & Straughan, B. (2020). Bidispersive thermal convection with relatively large macropores. *Journal of Fluid Mechanics*, 898, A14. doi: 10.1017/jfm.2020.411

[17] Anjali, D., Reddimalla, N., & Ramana Murthy, J.V. (2024). Unsteady flow of a couple stress fluid due to sudden withdrawal of pressure gradient in a parallel plate channel. *Archives of Thermodynamics*, 45(3), 179–184. doi: 10.24425/ather.2024.151220

[18] Mathews, J., & Hymavathi, T. (2024). Unsteady magnetohydrodynamic free convection and heat transfer flow of Al2O3–Cu/water nanofluid over a non-linear stretching sheet in a porous medium. *Archives of Thermodynamics*, 45(1), 165–173. doi: 10.24425/ather.2024.150449

[19] Jagadha, S., Madhusudhan Rao, B., Durgaprasad, P., Gopal, D., Prakash, P., Kishan, N., & Muthunagai, K. (2023). Darcy Forchheimer two-dimensional thin flow of Jeffrey nanofluid with heat generation/absorption and thermal radiation over a stretchable flat sheet. *Archives of Thermodynamics*, 45(2), 247-259. doi: 10.24425/ather.2024.150869